

WESPE: Weakly Supervised Photo Enhancer for Digital Cameras

Andrey Ignatov, Nikolay Kobyshev, Kenneth Vanhoey, Radu Timofte, Luc Van Gool

ETH Zurich

andrey.ignatoff@gmail.com, {nk, vanhoey, timofte, vangool}@vision.ee.ethz.ch

Abstract

Low-end and compact mobile cameras demonstrate limited photo quality mainly due to space, hardware and budget constraints. In this work, we propose a deep learning solution that translates photos taken by cameras with limited capabilities into DSLR-quality photos automatically. We tackle this problem by introducing a weakly supervised photo enhancer (WESPE) – a novel image-to-image Generative Adversarial Network-based architecture. The proposed model is trained by weakly supervised learning: unlike previous works, there is no need for strong supervision in the form of a large annotated dataset of aligned original/enhanced photo pairs. The sole requirement is two distinct datasets: one from the source camera, and one composed of arbitrary high-quality images that can be generally crawled from the Internet – the visual content they exhibit may be unrelated. Hence, our solution is repeatable for any camera: collecting the data and training can be achieved in a couple of hours. Our experiments on the DPED, Kitti and Cityscapes datasets as well as pictures from several generations of smartphones demonstrate that WESPE produces comparable qualitative results with state-of-the-art strongly supervised methods, while not requiring the tedious work to obtain aligned datasets.

1 Introduction

The ever-increasing quality of camera sensors allows us to photograph scenes with unprecedented detail and color. But as one gets used to better quality standards, photos captured just a few years ago with older hardware look dull and outdated. Analogously, despite incredible advancement in quality of images captured by mobile devices, compact sensors and lenses makes DSLR-quality unattainable for them, leaving casual users with a constant dilemma of relying on their lightweight mobile device or transporting a heavier-weight camera around on a daily basis. However, the second option may not be always possible for a number of other applications such as autonomous driving or video surveillance systems, where primitive cameras are usually employed.

In general, image enhancement can be done manually (e.g., by a graphical artist) or semi-automatically using specialized software capable of histogram equalization, photo sharpening, contrast adjustment, etc. The quality of the result in this case



Figure 1: Cityscapes image enhanced by our method.

significantly depends on user skills and allocated time, and thus is not doable by non-graphical experts on a daily basis, or not applicable in case of real-time or large-scale data processing. A fundamentally different option is to train various learning-based methods that allow to automatically transform image style or to perform image enhancement. Yet, one of the major bottlenecks of these solutions is the need for strong supervision using matched before/after training pairs of images. This requirement is often the source of a strong limitation of style transfer [25] and photo enhancement [14] methods. In the latter, a large dataset of paired images for specific camera models was acquired manually to overcome the problem.

In this paper, we present a novel weakly supervised solution for image enhancement problem to deliver ourselves from the above constraints. That is, we propose a deep learning architecture that can be trained to enhance images by mapping them from the domain of a given source camera into the domain of high-quality photos (supposedly taken by high-end DSLRs), while not requiring any correspondence or relation between the im-

ages from these domains: only two separate photo collections representing these domains are needed for training the network. To achieve this, we take advantage of two novel advancements in generative Convolutional Neural Networks (CNN): **i)** transitive CNNs to map the enhanced image back to the space of source images so as to relax the need of paired ground truth photos [45], and **ii)** loss functions combining color, content and texture loss to learn photorealistic image quality [14]. The major property of the method is that it can be learned easily: the training data is trivial to obtain for any camera and training takes just a few hours, hence it is sufficiently scalable to be readily trained and deployed for many cameras. Yet, quality-wise, our results still surpass traditional enhancers and compete with state of the art learning-based methods by producing artifact-less results.

Contributions. Enhanced images improve the non-enhanced ones in several aspects, including (but not limited to) colorization, resolution and sharpness. Our contributions can be summarized as follows:

- i. we provide WESPE, a generic method for learning a model that enhances images taken by a source camera to produce DSLR-quality results,
- ii. we define a transitive CNN GAN architecture suitable for the task of image enhancement and domain transfer by combining state of the art losses with a content loss expressed on the input image,
- iii. we provide experiments on several publicly available datasets with a variety of camera types, including a subjective user study and comparing to state of the art enhancement methods,
- iv. we make the model and the code openly available online¹, progressively augmenting it with additional camera models and types.

2 Related work

Automatic photo-enhancement can be considered as a typical computational photography task. To build our solution, we base upon three sub-fields: style transfer, image restoration and general-purpose image-to-image enhancers.

2.1 Style transfer

The goal of style transfer is to apply the style of one image to the (visual) content of another. Traditional texture/color/style transfer techniques [8, 25] rely on an exemplar before/after pair that defines the transfer to be applied: it is an aligned pair showing a similar scene in different styles. Thanks to dense pixel matching, this transfer is then applied to a target image. The exemplar pair is required to contain content sufficiently analogous to the target image, which is hard to find, and this hinders its automatic and mass usage.

More recently, neural style transfer alleviates this requirement [9, 31]. It builds on the assumption that the shallower layers of a deep CNN classifier characterize the style of an image, while the deeper ones represent semantic content. A neural network is then used to obtain an image matching the style of one input and the content of another.

Finally, generative adversarial networks (GAN) append a discriminator CNN to a generator network [11]. The role of the former is to distinguish between two domains of images: e.g., those having the style of the target image and those produced by the generator network. It is jointly trained with the generator, whose role is in turn to fool the discriminator by generating an image in the right domain, i.e., the domain of images of correct style. We exploit this logic to force the produced images to be in the domain of target high-quality photos.

2.2 Image restoration

Image quality enhancement has traditionally been addressed through a list of its sub-tasks, like super-resolution, deblurring, dehazing, denoising, colorization and image adjustment. Our goal of hallucinating high-end images from low-end ones encompasses all these enhancements. Many of these tasks have recently seen the arrival of successful methods driven by deep learning phrased as image-to-image translation problems. However, a common property of these works is that they are targeted at *restoring artifacts added artificially* to clean images. Such approaches require modeling of all possible distortions. Exhaustively modeling the flaws of the optics of one camera compared to a high-end reference one is close to impossible, let alone repeating this for a large list of camera pairs. Nevertheless, many useful ideas have emerged in these works, their brief review is given below.

The goal of *image super-resolution* is to restore the original image from its downsampled version. This problem is relevant to our task, as resolutions of DSLR cameras are generally higher than the ones of mobile devices. Many end-to-end CNN-based solutions exist now [7, 17, 27, 24]. Initial generative networks used pixel-wise mean-squared-error (MSE) loss functions, which often generated blurry results. Losses based on the activations of (a number of) VGG-layers [16] and GANs [19] are more capable of recovering photorealistic results, including high-frequency components, hence produce state of the art results.

Image colorization, which attempts to regress the 3 RGB channels from images that were reduced to single-channel grayscale, strongly benefits from the GAN architecture too [15]. Image *denoising*, *deblurring* and *dehazing* [42, 29, 13, 21, 4], *photographic style control* [34] and *transfer* [20], as well as *exposure correction* [39] are another improvements and adjustments that are included in our learned model. As opposed to mentioned related work, there is no need to manually model these effects in our case.

¹<http://people.ee.ethz.ch/~ihnatova/wespe.html>

2.3 General-purpose image-to-image enhancers

We build our solution upon very recent advances in image-to-image translation networks. Isola et al. [15] present a general-purpose translator that takes advantage of GANs to learn the loss function depending on the domain the target image should be in. While it achieves promising results when transferring between very different domains (e.g., aerial image to street map), it lacks photorealism when generating photos: results are often blurry and with strong checkerboard artifacts. Compared to our work, it needs *strong supervision*, in the form of many before/after examples provided at training time.

Zhu et al. [45] loosen this constraint by expressing the loss in the space of input rather than output images, taking advantage of a backward mapping CNN that transforms the output back into the space of input images. We apply a similar idea in this work. However, our CNN architecture and loss functions are based on different ideas: fully convolutional networks and complex losses allows us to achieve photorealistic results, while eliminating typical artifacts and limitations of encoder-decoder networks.

Finally, Ignatov et al. [14] propose an end-to-end enhancer achieving photorealistic results for arbitrary-sized images due to a composition of content, texture and color losses. However, it is trained with a strong supervision requirement. We build upon their loss functions to achieve photorealism as well, while adapting them to the new architecture suitable for our weakly supervised learning setting.

3 Proposed method

Our goal is to learn a mapping from a source domain X (e.g., defined by a low-end digital camera) to a target domain Y (e.g., defined by a collection of captured or crawled high-quality images). The inputs are unpaired training image samples $x \in X$ and $y \in Y$. As illustrated in Fig. 2, our model consists of a generative mapping $G : X \rightarrow Y$ paired with an inverse generative mapping $F : Y \rightarrow X$. VGG-19 features are computed for the original and reconstructed images x and \tilde{x} to measure content consistency between the mapping $G(x)$ and the input image x . Defining the *content loss* in the input image domain allows us to circumvent the need of before/after training pairs. Two adversarial discriminators D_c and D_t and total variation (TV) complete our loss definition. D_c aims to distinguish between high-quality image y and enhanced image $\tilde{y} = G(x)$ based on image colors, and D_t based on image texture. As a result, our objective comprises: i) content consistency loss to ensure G preserves x 's content, ii) two adversarial losses ensuring generated images \tilde{y} lie in the target domain Y : a color loss and a texture loss, and iii) TV loss to regularize towards smoother results.

3.1 Content consistency loss

We define the *content consistency loss* in the input image domain X : that is, on x and its reconstruction $\tilde{x} = F(\tilde{y}) = F(G(x))$ (inverse mapping from the enhanced image), as shown in Fig. 2. Our network is trained for both the direct G and inverse F map-

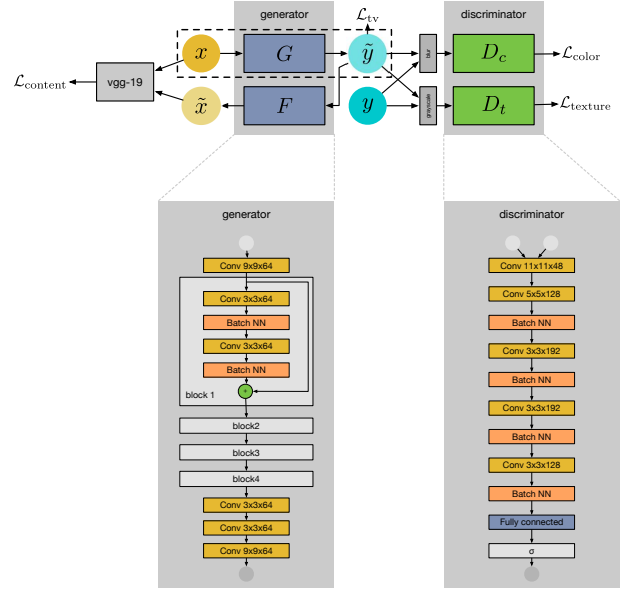


Figure 2: Proposed solution.

ping simultaneously, aiming at strong content similarity between the original and enhanced image. We found pixel-level losses too restrictive in this case, hence we choose a perceptual content loss based on ReLU activations of the VGG-19 network [28], inspired by [14, 16, 19]. It is defined as the l_2 -norm between feature representations of the input image x and the recovered image \tilde{x} :

$$\mathcal{L}_{\text{content}} = \frac{1}{C_j H_j W_j} \|\psi_j(x) - \psi_j(\tilde{x})\|, \quad (1)$$

where $\psi_j()$ is the feature map from the j -th VGG-19 convolutional layer and C_j , H_j and W_j are the number, height and width of the feature maps, respectively.

3.2 Adversarial color loss

Image color quality is measured using an adversarial discriminator D_c that is trained to differentiate between the blurred versions of enhanced \tilde{y}_b and high-quality y_b images:

$$y_b(i, j) = \sum_{k, l} y(i + k, j + l) \cdot G_{k, l}, \quad (2)$$

where $G_{k, l} = A \exp\left(-\frac{(k - \mu_x)^2}{2\sigma_x} - \frac{(l - \mu_y)^2}{2\sigma_y}\right)$ defines Gaussian blur with $A = 0.053$, $\mu_{x, y} = 0$, and $\sigma_{x, y} = 3$.

The main idea here is that the discriminator should learn the differences in brightness, contrast and major colors between low- and high-quality images, while it should avoid texture and content comparison. A constant σ was defined experimentally to be the smallest value that ensures texture and content eliminations. As a result, color loss forces the enhanced images to have similar color distribution as the target high-quality pictures. The loss itself is defined as a standard generator objective:

$$\mathcal{L}_{\text{color}} = - \sum_i \log D_c(G(x)_b). \quad (3)$$



Figure 3: From left to right, top to bottom: original iPhone 3GS photo and the same image after applying, resp.: Apple Photo Enhancer, WESPE trained on DPED, WESPE trained on DIV2K, Ignatov et al. [14], and the corresponding DSLR image.

3.3 Adversarial texture loss

Similarly to color, image texture quality is also assessed by an adversarial discriminator D_t that is applied to grayscale images and is trained to predict whether the input one was enhanced (\tilde{y}_g) or is a “true” high-quality image (y_g). As in the previous case, the network is trained to minimize the cross-entropy loss function, the loss is defined as:

$$\mathcal{L}_{\text{texture}} = - \sum_i \log D_t(G(x)_g). \quad (4)$$

3.4 TV loss

To impose spatial smoothness of the generated images we also add a total variation loss [2] defined as follows:

$$\mathcal{L}_{\text{tv}} = \frac{1}{CHW} \|\nabla_x G(x) + \nabla_y G(x)\|, \quad (5)$$

where C , H and W are the dimensions of the generated image $G(x)$.

3.5 Total loss

Our final objective loss is the linear combination of the four previously introduced losses with the following weights:

$$\mathcal{L}_{\text{total}} = \mathcal{L}_{\text{content}} + 5 \cdot 10^{-3} (\mathcal{L}_{\text{color}} + \mathcal{L}_{\text{texture}}) + 10 \mathcal{L}_{\text{tv}}. \quad (6)$$

The weights were picked based on preliminary experiments on our training data.

3.6 Network architecture and training details

The overall architecture of the system is illustrated in Fig. 2. Both generative and inverse generative networks G and F are fully-convolutional residual CNNs with four residual blocks, their architecture was adapted from [14]. The discriminator CNNs consist of five convolutional and one fully-connected layer with 1024 neurons, followed by the last layer with sigmoidal activation function on top of it. The first, second and fifth convolutional layers are strided with a step size of 4, 2 and 2, respectively.

The network was trained on *Nvidia Titan X* GPU for 20K iterations using a batch size of 30, the size of the input patches was 100×100 pixels. The parameters of the networks were optimized using Adam algorithm, the experimental setup was identical in all experiments.

4 Experiments

We apply the proposed network to different datasets and compare quantitatively and qualitatively (through a user study) against a baseline (the Apple Photos image enhancement software, or APE) and the most recent and state of the art related work of Ignatov et al. [14] that exploits full supervision.

4.1 Image quality assessment

In our experiments, we used full-reference pixel-wise measures when applicable, i.e., when ground truth enhanced images are available. Point Signal-to-Noise Ratio (**PSNR**) measures the



Figure 4: Original (top) vs. WESPE [DIV2K] enhanced (bottom) DPED images captured by BlackBerry and Sony cameras.

Table 1: Average PSNR, SSIM, entropy and bit per pixel results on DPED test images. WESPE is trained either on DPED or on DIV2K dataset.

Phone	APE				Weakly supervised								Fully supervised			
					WESPE trained on DIV2K				WESPE trained on DPED				[14] trained on DPED			
	PSNR	SSIM	entr.	bpp	PSNR	SSIM	entr.	bpp	PSNR	SSIM	entr.	bpp	PSNR	SSIM	entr.	bpp
iPhone	17.28	0.86	7.39	9.33	18.85	0.87	7.59	12.29	19.74	0.90	7.57	10.68	21.35	0.92	7.62	11.07
BlackBerry	18.91	0.89	7.55	10.19	18.42	0.90	7.59	11.36	19.00	0.92	7.55	10.32	20.66	0.93	7.63	9.98
Sony	19.45	0.92	7.62	11.37	20.83	0.89	7.50	11.72	21.93	0.93	7.63	11.19	22.01	0.94	7.64	10.99

amount of signal lost wrt a reference, hence helps us quantify how close we are to it. **SSIM** [33] measures the structural similarity with the reference and is known to correlate better with human perception than PSNR. Codebook Representation for No-Reference Image Assessment (**CORNIA**) [37] is a perceptual measure mapping to average human quality assessments. Complementarily, we compute image **entropy** (based on pixel level observations) and bit per pixel (**bpp**) of the PNG lossless image compression. Both entropy and bpp are indicators of the quantity of image information. Since the final aim of our work is to improve both the quality and the aesthetics of an input image we also conduct a user study.

4.2 Weakly vs. fully supervised learning

[14] proposed a photo enhancer learned with full supervision on the DPED dataset composed of pixel-aligned pairs of source and target images. It contains images from 3 smartphones with low-to middle-end cameras (iPhone 3Gs, BlackBerry Passport and Sony Xperia Z) paired with images of the same scenes taken by a high-end DSLR camera (Canon 70D). Thanks to pixel-aligned ground truth high-quality images, we can use this data to evaluate our method using the pixel-wise image quality metrics (PSNR and SSIM).

We adhere to the same setup and train our model for mapping from the smartphone image source domain to the DSLR target

domain. Note that we use the target images in weak supervision: only for training the adversarial discriminators and not for pixel level losses as in [14]. We train 2 networks with different target images: the first uses the original DPED DSLR photos as target, while the second uses high-quality pictures from DIV2K [1] dataset.

PSNR, SSIM, bpp and image entropy are given in Table 1. Our WESPE network trained with the DPED DSLR target performs better than the APE and almost as good as the network [14] that uses a fully supervised approach and requires pixel-aligned ground truth. Numerical evaluation of our network trained to target DIV2K images performs worse on PSNR and SSIM. This is because these metrics take DSLR image as a reference, and even minor difference of colors between the resulting image and the compared DSLR reference can worsen the score. The resulting pictures trained on DIV2K have more crisp colors compared to WESPE trained on DSLR (see Fig. 3) and very high bpp scores. This shows that training benefits from a data diverse dataset (different sources) of high-quality images with little noise levels, rather than a set of images from a single high-quality camera. More results are shown in Fig. 4.

4.3 Training on unsupervised datasets

While the DPED dataset contains pictures from mostly old phones, we have collected a complementary dataset of pictures

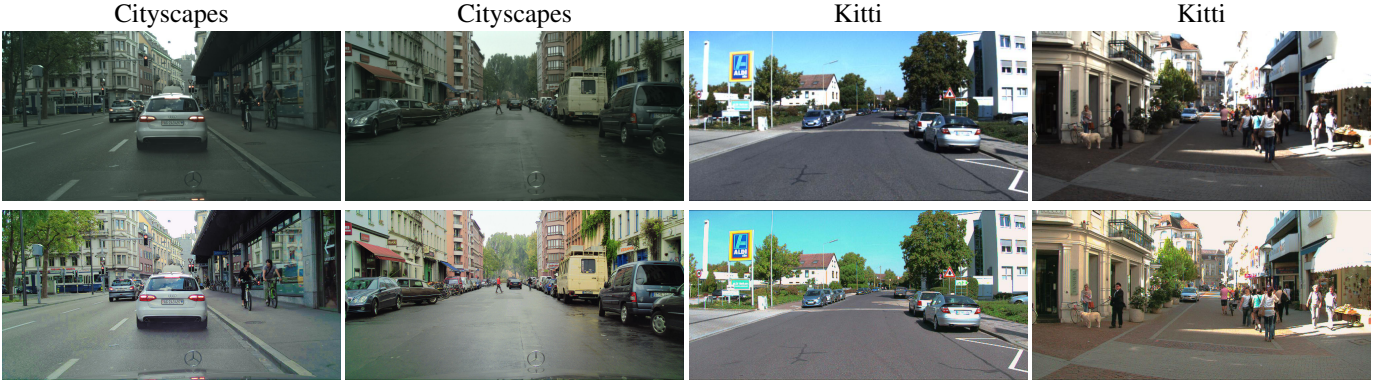


Figure 5: Examples of original (top) vs. enhanced (bottom) images for Cityscapes and Kitti dataset.

images	original			WESPE enhanced			APE		
	entropy	bpp	CORNIA	entropy	bpp	CORNIA	entropy	bpp	CORNIA
Cityscapes	6.72	5.03	46.56	7.55	12.04	28.92	7.30	6.74	46.73
KITTI	7.29	10.06	39.40	7.62	13.56	32.22	7.58	10.21	37.64
HTC	7.51	8.30	27.33	7.73	11.50	29.91	7.64	9.64	28.46
Huawei	7.71	9.30	25.84	7.77	11.63	29.89	7.78	10.27	25.85
iPhone	7.56	8.04	30.88	7.56	10.08	36.06	7.57	9.25	35.82

Table 2: Results on the fully unsupervised 5 datasets

taken by phones that are marketed to have state-of-the-art cameras: iPhone 6, HTC One M9 and Huawei P9. As images found online may suffer from additional compression artifacts, we did a manual collection ourselves. For each phone, the dataset consists of approximately 1500 pictures. We additionally use the Cityscapes [6] and KITTI [10] datasets to evaluate the performance of the network on public datasets that contain images of low quality. In the following experiments, we use DIV2K images as target as it has shown better performance on DPED dataset. We compute image entropy and bpp (which is correlated with information quantity) and CORNIA (where lower is better) for original, WESPE-enhanced, and baseline(APE)-enhanced images. Results are shown in Table 2.

For the city datasets (Kitti and Cityscapes), our method demonstrates significantly better results on CORNIA and bits per pixel, and also scores higher on image entropy. The city datasets consist of images of poor quality, and our method is successful in healing such pictures. On the phones, our method shows better results on bits per pixel, worse scores on CORNIA, keeping image entropy on the same level. Since these results are quite ambiguous, a complementary user study for subjective quality evaluation is performed in section 4.4. Visual results for the city datasets and phones are shown in Fig. 5 and 6.

4.4 Subjective qualitative evaluation

Numerical results are not necessarily correlated to human perception. Hence, we have additionally conducted a user study to verify our findings. 38 people chose their preferred among 2 pictures displayed side by side. No additional selection criteria were specified, and users were allowed to zoom in and out at

will without time restriction. The study consisted of 7 pairs of pictures before and after applying our method for each dataset (which sums to 35 questions for 3 modern phones and 2 city datasets) and 7 pairs of improved pictures using our method and APE (another 35 questions). The question sequence, as well as the sequence of pictures in each pair, were randomized for each user. Results are shown in Table 3.

WESPE-improved images are consistently preferred over non-enhanced images, even strongly for most datasets. It is also often preferred over APE, strongly on KITTI and especially on Cityscapes dataset, while for the Huawei P9 phone the results are comparable.

5 Conclusion

In this work, we presented WESPE – a weakly supervised solution for the image quality enhancement problem. In contrast to previously proposed approaches that required strong supervision in the form of aligned source-target training image pairs, this method is free of this limitation. That is, it is trained to map low-quality photos into the domain of high-quality photos without requiring any correspondence between them: only two separate photo collections representing these domains are needed. To solve the problem, we proposed a transitive architecture that is based on Generative Adversarial Networks and loss functions designed for high-quality image quality assessment. The method was validated on several publicly available datasets with different camera types. Our experiments reveal that WESPE demonstrates the performance comparable or surpassing the traditional enhancers, and gets close or competes with the current state of



Figure 6: Original (top) vs. enhanced (bottom) images for iPhone, HTC and Huawei cameras.

the art supervised methods, while relaxing the need of supervision thus avoiding tedious creation of pixel-aligned datasets.

References

- [1] E. Agustsson and R. Timofte. Ntire 2017 challenge on single image super-resolution: Dataset and study. In *The IEEE Conference on Computer Vision and Pattern Recognition (CVPR) Workshops*, July 2017. 5
- [2] H. A. Aly and E. Dubois. Image up-sampling using total-variation regularization with a new observation model. *IEEE Transactions on Image Processing*, 14(10):1647–1659, Oct 2005. 4
- [3] C. Barnes, E. Shechtman, D. B. Goldman, and A. Finkelstein. The generalized PatchMatch correspondence algorithm. In *European Conference on Computer Vision*, Sept. 2010.
- [4] B. Cai, X. Xu, K. Jia, C. Qing, and D. Tao. Dehazenet: An end-to-end system for single image haze removal. *IEEE Transactions on Image Processing*, 25(11):5187–5198, Nov 2016. 2
- [5] Z. Cheng, Q. Yang, and B. Sheng. Deep colorization. In *The IEEE International Conference on Computer Vision (ICCV)*, December 2015.
- [6] M. Cordts, M. Omran, S. Ramos, T. Rehfeld, M. Enzweiler, R. Benenson, U. Franke, S. Roth, and B. Schiele. The cityscapes dataset for semantic urban scene understanding. In *Proc. of the IEEE Conference on Computer Vision and Pattern Recognition (CVPR)*, 2016. 6
- [7] C. Dong, C. C. Loy, K. He, and X. Tang. *Learning a Deep Convolutional Network for Image Super-Resolution*, pages 184–199. Springer International Publishing, Cham, 2014. 2
- [8] A. A. Efros and W. T. Freeman. Image quilting for texture synthesis and transfer. In *Proceedings of the 28th Annual Conference on Computer Graphics and Interactive Techniques, SIGGRAPH '01*, pages 341–346, New York, NY, USA, 2001. ACM. 2
- [9] L. A. Gatys, A. S. Ecker, and M. Bethge. A neural algorithm of artistic style. *CoRR*, abs/1508.06576, 2015. 2
- [10] A. Geiger, P. Lenz, and R. Urtasun. Are we ready for autonomous driving? the kitti vision benchmark suite. In *Conference on Computer Vision and Pattern Recognition (CVPR)*, 2012. 6
- [11] I. Goodfellow, J. Pouget-Abadie, M. Mirza, B. Xu, D. Warde-Farley, S. Ozair, A. Courville, and Y. Bengio. Generative adversarial nets. In Z. Ghahramani, M. Welling, C. Cortes, N. D. Lawrence, and K. Q. Weinberger, editors, *Advances in Neural Information Processing Systems 27*, pages 2672–2680. Curran Associates, Inc., 2014. 2
- [12] A. Hertzmann, C. E. Jacobs, N. Oliver, B. Curless, and D. H. Salesin. Image analogies. In *Proceedings of the 28th Annual Conference on Computer Graphics and Interactive Techniques, SIGGRAPH '01*, pages 327–340, New York, NY, USA, 2001. ACM.
- [13] M. Hradiš, J. Kotera, P. Zemčák, and F. Šroubek. Convolutional neural networks for direct text deblurring. In *Proceedings of BMVC 2015*. The British Machine Vision Association and Society for Pattern Recognition, 2015. 2
- [14] A. Ignatov, N. Kobyshev, K. Vanhoey, R. Timofte, and L. V. Gool. Dslr-quality photos on mobile devices with

- deep convolutional networks. *CoRR*, abs/1704.02470, 2017. **1, 2, 3, 4, 5**
- [15] P. Isola, J.-Y. Zhu, T. Zhou, and A. A. Efros. Image-to-image translation with conditional adversarial networks. *arxiv*, 2016. **2, 3**
- [16] J. Johnson, A. Alahi, and L. Fei-Fei. *Perceptual Losses for Real-Time Style Transfer and Super-Resolution*, pages 694–711. Springer International Publishing, Cham, 2016. **2, 3**
- [17] J. Kim, J. K. Lee, and K. M. Lee. Accurate image super-resolution using very deep convolutional networks. In *2016 IEEE Conference on Computer Vision and Pattern Recognition (CVPR)*, pages 1646–1654, June 2016. **2**
- [18] D. P. Kingma and J. Ba. Adam: A method for stochastic optimization. *CoRR*, abs/1412.6980, 2014.
- [19] C. Ledig, L. Theis, F. Huszar, J. Caballero, A. P. Aitken, A. Tejani, J. Totz, Z. Wang, and W. Shi. Photo-realistic single image super-resolution using a generative adversarial network. *CoRR*, abs/1609.04802, 2016. **2, 3**
- [20] J.-Y. Lee, K. Sunkavalli, Z. Lin, X. Shen, and I. So Kweon. Automatic content-aware color and tone stylization. In *The IEEE Conference on Computer Vision and Pattern Recognition (CVPR)*, June 2016. **2**
- [21] Z. Ling, G. Fan, Y. Wang, and X. Lu. Learning deep transmission network for single image dehazing. In *2016 IEEE International Conference on Image Processing (ICIP)*, pages 2296–2300, Sept 2016. **2**
- [22] D. G. Lowe. Distinctive image features from scale-invariant keypoints. *International Journal of Computer Vision*, 60(2):91–110, 2004.
- [23] F. Luan, S. Paris, E. Shechtman, and K. Bala. Deep photo style transfer. *CoRR*, abs/1703.07511, 2017.
- [24] X. Mao, C. Shen, and Y.-B. Yang. Image restoration using very deep convolutional encoder-decoder networks with symmetric skip connections. In D. D. Lee, M. Sugiyama, U. V. Luxburg, I. Guyon, and R. Garnett, editors, *Advances in Neural Information Processing Systems 29*, pages 2802–2810. Curran Associates, Inc., 2016. **2**
- [25] F. Okura, K. Vanhoey, A. Bousseau, A. A. Efros, and G. Drettakis. Unifying Color and Texture Transfer for Predictive Appearance Manipulation. *Computer Graphics Forum*, 2015. **1, 2**
- [26] W. Ren, S. Liu, H. Zhang, J. Pan, X. Cao, and M.-H. Yang. *Single Image Dehazing via Multi-scale Convolutional Neural Networks*, pages 154–169. Springer International Publishing, Cham, 2016.
- [27] W. Shi, J. Caballero, F. Huszar, J. Totz, A. P. Aitken, R. Bishop, D. Rueckert, and Z. Wang. Real-time single image and video super-resolution using an efficient sub-pixel convolutional neural network. In *The IEEE Conference on Computer Vision and Pattern Recognition (CVPR)*, June 2016. **2**
- [28] K. Simonyan and A. Zisserman. Very deep convolutional networks for large-scale image recognition. *arXiv preprint arXiv:1409.1556*, 2014. **3**
- [29] P. Svoboda, M. Hradis, D. Barina, and P. Zemčík. Compression artifacts removal using convolutional neural networks. *CoRR*, abs/1605.00366, 2016. **2**
- [30] R. Timofte, V. DeSmet, and L. VanGool. *A+: Adjusted Anchored Neighborhood Regression for Fast Super-Resolution*, pages 111–126. Springer International Publishing, Cham, 2015.
- [31] D. Ulyanov, V. Lebedev, A. Vedaldi, and V. S. Lempitsky. Texture networks: Feed-forward synthesis of textures and stylized images. *CoRR*, abs/1603.03417, 2016. **2**
- [32] A. Vedaldi and B. Fulkerson. VLFeat: An open and portable library of computer vision algorithms, 2008.
- [33] Z. Wang, A. C. Bovik, H. R. Sheikh, and E. P. Simoncelli. Image quality assessment: from error visibility to structural similarity. *IEEE Transactions on Image Processing*, 13(4):600–612, April 2004. **5**
- [34] Z. Yan, H. Zhang, B. Wang, S. Paris, and Y. Yu. Automatic photo adjustment using deep neural networks. *ACM Trans. Graph.*, 35(2):11:1–11:15, Feb. 2016. **2**
- [35] C. Yang, X. Lu, Z. Lin, E. Shechtman, O. Wang, and H. Li. High-resolution image inpainting using multi-scale neural patch synthesis. *CoRR*, abs/1611.09969, 2016.
- [36] W. Yang, R. T. Tan, J. Feng, J. Liu, Z. Guo, and S. Yan. Joint rain detection and removal via iterative region dependent multi-task learning. *CoRR*, abs/1609.07769, 2016.
- [37] P. Ye, J. Kumar, L. Kang, and D. Doermann. Unsupervised feature learning framework for no-reference image quality assessment. In *Computer Vision and Pattern Recognition (CVPR), 2012 IEEE Conference on*, pages 1098–1105. IEEE, 2012. **5**
- [38] P. Ye, J. Kumar, L. Kang, and D. Doermann. Unsupervised feature learning framework for no-reference image quality assessment. In *Computer Vision and Pattern Recognition (CVPR), 2012 IEEE Conference on*, pages 1098–1105. IEEE, 2012.
- [39] L. Yuan and J. Sun. *Automatic Exposure Correction of Consumer Photographs*, pages 771–785. Springer Berlin Heidelberg, Berlin, Heidelberg, 2012. **2**
- [40] K. Zhang, W. Zuo, Y. Chen, D. Meng, and L. Zhang. Beyond a gaussian denoiser: Residual learning of deep CNN for image denoising. *CoRR*, abs/1608.03981, 2016.

Table 3: Subjective evaluation result. We show the fraction of times our result was preferred over the non-enhanced image or the APE-enhanced image, respectively. Datasets comprise iPhone 6 (IPH), HTC One M9 (HTC), Huawei P9 (HW), Cityscapes (CS) and KITTI, respectively. Our result is nearly always preferred (boldface).

Dataset	IPH	HTC	HW	CS	KITTI
Prop. vs init.	0.70	0.73	0.63	0.94	0.81
Prop. vs APE	0.62	0.53	0.44	0.96	0.65

- [41] R. Zhang, P. Isola, and A. A. Efros. Colorful image colorization. *ECCV*, 2016.
- [42] X. Zhang and R. Wu. Fast depth image denoising and enhancement using a deep convolutional network. In *2016 IEEE International Conference on Acoustics, Speech and Signal Processing (ICASSP)*, pages 2499–2503, March 2016. 2
- [43] E. Zhou, H. Fan, Z. Cao, Y. Jiang, and Q. Yin. Learning face hallucination in the wild. In *Proceedings of the Twenty-Ninth AAAI Conference on Artificial Intelligence, AAAI’15*, pages 3871–3877. AAAI Press, 2015.
- [44] J.-Y. Zhu, P. Krähenbühl, E. Shechtman, and A. A. Efros. *Generative Visual Manipulation on the Natural Image Manifold*, pages 597–613. Springer International Publishing, Cham, 2016.
- [45] J.-Y. Zhu, T. Park, P. Isola, and A. A. Efros. Unpaired image-to-image translation using cycle-consistent adversarial networks. *arXiv preprint arXiv:1703.10593*, 2017. 2, 3